

Kinetics and Mechanism of the Cobalt Phthalocyanine Catalyzed Reduction of Nitrite and Nitrate by Dithionite in Aqueous Solution

Evgeny V. Kudrik,^{*,†,‡} Sergei V. Makarov,^{†,‡} Achim Zahl,[†] and Rudi van Eldik^{*,†}*Institute for Inorganic Chemistry, University of Erlangen-Nürnberg, Egerlandstrasse 1, 91058 Erlangen, Germany, and Ivanovo State University of Chemistry and Technology, av. F. Engels 7, 153460 Ivanovo, Russia*

Received April 22, 2002

The reaction of sodium nitrite with sodium dithionite was studied in the presence of cobalt(II) tetrasulfophthalocyanine, $\text{Co}^{\text{II}}(\text{TSPc})^{4-}$, in aqueous alkaline solution. The overall mechanism comprises the reduction of $\text{Co}^{\text{II}}(\text{TSPc})^{4-}$ by dithionite, followed by the formation of an intermediate complex between $\text{Co}^{\text{I}}(\text{TSPc})^{5-}$ and nitrite, which undergoes two parallel subsequent reactions with and without nitrite as a reagent. Kinetic parameters for the different reaction steps of the catalytic process were determined. The final product of the reaction was found to be ammonia. Contrary to those found for the catalytic reduction of nitrite, the products of the catalytic reduction of nitrate were found to be dinitrogen and nitrous oxide. The possible catalytic reduction of nitrous oxide was confirmed by independent experiments. The striking differences in the reduction products of nitrite and nitrate are explained in terms of different structures of the intermediate complex between $\text{Co}^{\text{I}}(\text{TSPc})^{5-}$ and substrate, in which nitrite and nitrate are suggested to coordinate via nitrogen and oxygen, respectively.

Introduction

Denitrification plays a key role in the biogeochemical nitrogen cycle.¹ Nitrate serves as the substrate for this process in which it is reduced via nitrite, nitric oxide, and nitrous oxide to dinitrogen. The first step, reduction of nitrate to nitrite, is catalyzed in organisms by molybdenum-containing enzymes, viz., nitrate reductases.² Since nitrate is a potentially harmful compound to human health,³ processes for nitrate removal from drinking water have regained interest in recent years.⁴ One of the most promising methods is catalytic nitrate reduction using bimetallic palladium catalysts.⁴

Reduction of nitrite is catalyzed in organisms by enzymes of two types. The first type is heme enzymes in which Fe^{II} is the active center in the porphyrin macrocycle. The second type involves enzymes containing Cu^{I} , viz., nitrite and nitric oxide reductases.⁵ Since reduction of nitrite represents the

branching point in assimilatory nitrate reduction,⁶ this process has received substantial attention in recent years. In addition to extensive studies of the biological denitrification process,⁶ the kinetics of the chemical reduction of nitrite by metallic iron,⁷ $\text{Fe}^{\text{II}}(\text{edta})$,⁸ amine–borane,⁹ and hydrazine¹⁰ has been studied in detail. Despite this progress, considerable controversy exists concerning the mechanisms of nitrite reduction. One of the unsettled questions is the role of nitric oxide.⁶ Is it an intermediate in the reduction of nitrite to N_2O , or is the formation of nitrous oxide a result of the reaction between nitrite and a product of its one-electron reduction reaction? Further interest in the redox reactions of N_2O was stimulated by reports of its greenhouse gas properties.¹¹ N_2O can account for as much as 7% of the projected atmospheric warming.¹²

* Authors to whom correspondence should be addressed. E-mail: ttos@isuct.ru (E.V.K.); vaneldik@chemie.uni-erlangen.de (R.v.E.).

† University of Erlangen-Nürnberg.

‡ Ivanovo State University of Chemistry and Technology.

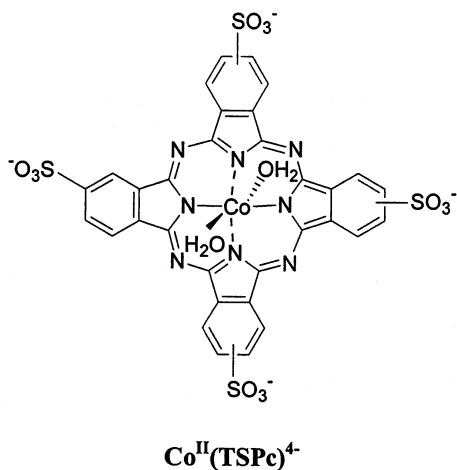
- (1) Richardson, D. J. *Cell. Mol. Life Sci.* **2001**, *58*, 163.
- (2) Campbell, W. H. *Annu. Rev. Plant Physiol. Plant. Mol. Biol.* **1999**, *50*, 277.
- (3) Haghghi, B.; Tavassoli, A. *Fresenius' J. Anal. Chem.* **2001**, *371*, 1113.
- (4) Prusse, U.; Vorlop, K.-D. *J. Mol. Catal., A: Chem.* **2001**, *173*, 313.
- (5) Wang, Y.; Averill, B. A. *J. Am. Chem. Soc.* **1996**, *118*, 3972.

- (6) Averill, B. A. *Chem. Rev.* **1996**, *96*, 2951.
- (7) Hu, H.-Y.; Goto, N.; Fujie, K. *Water Res.* **2001**, *35*, 2789.
- (8) Zang, V.; Kotowski, M.; van Eldik, R. *Inorg. Chem.* **1988**, *27*, 3279.
- (9) Bell, K. E.; Kelly, H. C. *Inorg. Chem.* **1996**, *35*, 7225.
- (10) Chevalier, A. A.; Gentil, L. A.; Amorebieta, V. T.; Gutierrez, M. M.; Olabe, J. A. *J. Am. Chem. Soc.* **2000**, *122*, 11238.
- (11) (a) Rasmussen, R. A.; Khalil, M. A. K. *Science* **1986**, *232*, 1623. (b) IPCC. *In Climate Change 1995, the Science of Climate Change*; Houghton, J. T., Meira Filho, L. G., Callander, B. A., Harris, N., Kattenberg, A., Maskell, K., Eds.; Cambridge University Press: Cambridge, U.K., 1996; pp 9–50. (c) Cicerone, R. J. *Science* **1987**, *237*, 35.
- (12) Smart, D. R.; Bloom, A. J. *Proc. Natl. Acad. Sci. U.S.A.* **2001**, *98*, 7875.

In addition, photolysis of N_2O in the upper atmosphere leads to ozone destruction.¹²

Two- and three-electron reduction processes of N_2O have been reported.^{13,14} In both reactions nitrous oxide reacts with low-valence metal complexes. For this purpose the low-valence metal complex should be relatively stable. A promising candidate is cobalt phthalocyanine, $\text{Co}(\text{Pc})$. According to DFT calculations,¹⁵ the electron received during reduction of $\text{Co}^{\text{II}}(\text{Pc})$ is localized on the metal center and not on the ligand as in the case of the phthalocyanine complexes of Cu, Ni, and Zn. This illustrates the relative stability of $\text{Co}^{\text{I}}(\text{Pc})$. Another advantage of cobalt phthalocyanine is that complexes of $\text{Co}^{\text{I}}(\text{Pc})$, soluble in water and in organic solvents, may be synthesized from commercially available $\text{Co}^{\text{II}}(\text{Pc})$ derivatives. For this purpose electrochemical¹⁶ and pulse radiolysis¹⁷ techniques, or reduction with sodium in THF,¹⁷ have been used. Cobalt(I) phthalocyanine is shown to be stable in alkaline solutions for at least several hours.¹⁷

In this study, we prepared cobalt(I) tetrasulfophthalocyanine, $\text{Co}^{\text{I}}(\text{TSPc})^{5-}$ via reduction of $\text{Co}^{\text{II}}(\text{TSPc})^{4-}$ with sodium dithionite. Subsequently, we used $\text{Co}^{\text{I}}(\text{TSPc})^{5-}$ as a catalyst for the reduction of nitrite and nitrate in alkaline solution. The kinetics and mechanisms of these reactions were studied in detail.



Experimental Section

Materials. Sodium nitrate, sodium nitrite, and sodium dithionite (93% grade) were obtained from Aldrich and used as received. Nitrous oxide was supplied by Linde. $\text{Co}^{\text{II}}(\text{TSPc})^{4-}$ was prepared and purified using a literature method.¹⁸ Boric acid/potassium chloride/sodium hydroxide, TRICINE, CHES, and CAPS buffers were used to control the pH. $\text{Na}^{15}\text{NO}_2$ (95% ^{15}N grade) and K^{15}NO_3

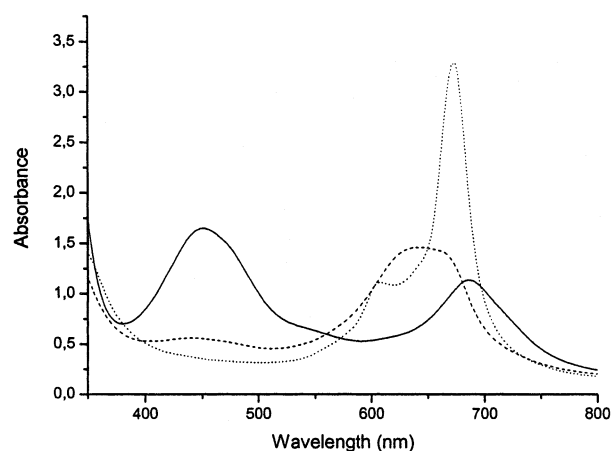


Figure 1. Visible absorbance spectra of different forms of $\text{Co}(\text{TSPc})$ at pH 10: $\text{Co}^{\text{I}}(\text{TSPc})^{4-}$ (7.8×10^{-5} M, solid line), $\text{Co}^{\text{I}}(\text{TSPc})^{5-}$ after reaction with NO_2^- (7.8×10^{-5} M, dashed line), $\text{Co}^{\text{III}}(\text{TSPc})^{4-}$ prepared from a reaction of $\text{Co}^{\text{II}}(\text{TSPc})^{4-}$ with sulfite in the presence of oxygen (4.4×10^{-5} M, dotted line).

(96% ^{15}N grade) were used for ^{15}N NMR and MS analyses. Oxygen-free argon was used to deoxygenate solutions.

Kinetic Measurements and Instrumentation. Conventional kinetic experiments were performed on a Cary 1 or Cary 5 UV-vis spectrophotometer under anaerobic conditions. No salt was added to control the ionic strength. The data were analyzed using Origin 6.1 and SPECFIT software. A thermostated (± 0.1 °C) Applied Photophysics SX 18MV stopped-flow spectrophotometer with an observation path length of 1.0 cm was used to follow the faster reactions. NMR measurements were performed using a Bruker Avance DRX400 WB spectrometer equipped with a superconducting BS-94/89 magnet system, at 40.56 MHz for ^{15}N and 400.13 MHz for ^1H . ^{15}N chemical shifts were referenced externally to neat nitromethane. D_2O (99%) was used for all measurements. Mass spectra were recorded on a JEOL Mstation 700 (EI, 70 eV) spectrometer. EPR spectra were recorded on a Bruker ESP 300 E spectrometer (9.96 GHz) in H_2O at 177 K.

Results and Discussion

Reaction of Sodium Dithionite with Cobalt(II) Tetrasulfophthalocyanine. Reduction of a $\text{Co}^{\text{II}}(\text{TSPc})^{4-}$ solution by excess sodium dithionite is accompanied by a color change from blue to brown. An intensive absorption maximum appears at 450 nm in the UV-vis spectrum, and simultaneously the Q-band is shifted to the red region (Figure 1).

This spectrum differs considerably from that for $\text{Co}^{\text{III}}(\text{TSPc})^{3-}$ and is essentially identical to that reported for $\text{Co}^{\text{I}}(\text{TSPc})^{5-}$.⁵⁻¹⁷ The rate of reduction of $\text{Co}^{\text{II}}(\text{TSPc})^{4-}$ was found to be independent of the $\text{Co}^{\text{II}}(\text{TSPc})^{4-}$ concentration. Rate constants determined from the increase in the absorbance maximum at 450 nm (viz., 2.2 ± 0.1 s $^{-1}$ at 25 °C) are in close agreement with that reported for the dissociation of dithionite in reaction 1, viz., 2.5 s $^{-1}$ at 25 °C.¹⁹ This suggests that reaction 1 is clearly the rate-determining step, which is followed by the rapid reduction of $\text{Co}^{\text{II}}(\text{TSPc})^{4-}$ by the sulfur dioxide anion radical in reaction 2.

- (13) Groves, J. T.; Roman, J. S. *J. Am. Chem. Soc.* **1995**, *117*, 5594.
 (14) Cherry, J.-P. F.; Johnson, A. R.; Baraldo, L. M.; Tsai, Y.-C.; Cummins, C. C.; Kryatov, S. V.; Rybak-Akimova, E. V.; Capps, K. B.; Hoff, C. D.; Haar, C. M.; Nolan, S. P. *J. Am. Chem. Soc.* **2001**, *123*, 7271.
 (15) Liao, M. S.; Scheiner, S. *J. Chem. Phys.* **2001**, *114*, 9780.
 (16) Meshisuka, S.; Ichikawa, M.; Tamaru, K. *J. Chem. Soc., Chem. Commun.* **1975**, *9*, 360.
 (17) Grodkowski, J.; Dhanasekaran, T.; Neta, P.; Hambright, P.; Brunschwig, B. S.; Shinozaki, K.; Fujita, E. *J. Phys. Chem. A* **2000**, *104*, 11332.
 (18) (a) Weber, J. N.; Busch, D. H. *Inorg. Chem.* **1965**, *4*, 469. (b) Yang, Y.-C.; Ward, R. J.; Seiders, R. P. *Inorg. Chem.* **1985**, *24*, 1765.

- (19) Creutz, C.; Sutin, N. *Inorg. Chem.* **1974**, *13*, 4041.

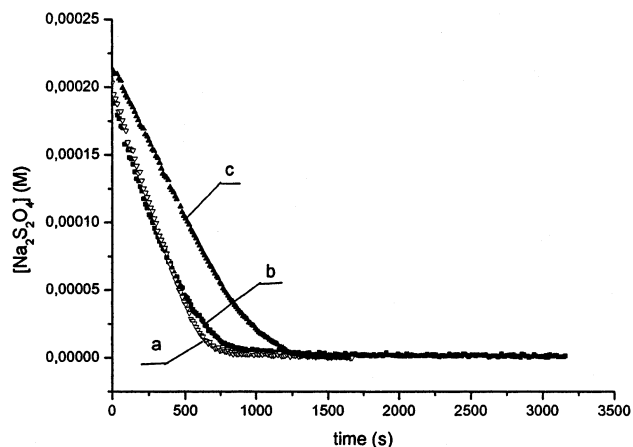
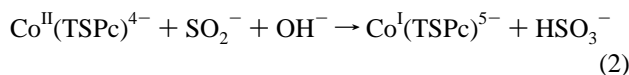


Figure 2. Time dependence of $[\text{Na}_2\text{S}_2\text{O}_4]$ during the reaction of NaNO_2 with $\text{Na}_2\text{S}_2\text{O}_4$ in the presence of $\text{Co}^{\text{II}}(\text{TSPc})^{4-}$, $[\text{NaNO}_2] = 3.5 \times 10^{-2} \text{ M}$, $[\text{Co}^{\text{II}}(\text{TSPc})^{4-}] = 7.8 \times 10^{-5}$ (a), 5.2×10^{-5} (b), and 2.6×10^{-5} (c) M, pH 10, 25 °C.



Since $\text{Co}^{\text{I}}(\text{TSPc})^{5-}$ is diamagnetic, ^1H NMR spectroscopy was used to study its structure in solution. Chemical shifts in the range 7.82–7.39 ppm (see Figure S1, Supporting Information) correspond to the 12 protons of the isoindole fragments. The ^1H NMR spectrum indicates that the $\text{Co}^{\text{I}}(\text{TSPc})^{5-}$ complex is a mixture of four regioisomers. It should, however, be noted that the mentioned signals are upfield shifted in comparison to those reported for other tetrasubstituted phthalocyanines,²⁰ probably due to distortion of the planar structure of the macrocycle as a result of an increase in the covalent radius of the central metal cation.

Reaction of Sodium Dithionite with Sodium Nitrite in the Presence of Cobalt Tetrasulphthalocyanine. Preliminary experiments showed that the direct reaction between dithionite and nitrite did not proceed with measurable rates under conditions employed in this study (i.e., pH 10, 15–50 °C). During the investigation of reactions catalyzed by cobalt(II) tetrasulphthalocyanine, we found that the absorbance observed at 315 nm did not depend on the oxidation state of the cobalt complex. Although nitrite also absorbs at 315 nm, its molar absorbance coefficient ($11 \text{ M}^{-1} \text{ cm}^{-1}$) is much less than for dithionite²¹ ($8043 \text{ M}^{-1} \text{ cm}^{-1}$). Since NaNO_2 was used in excess, changes in its absorbance at 315 nm during the reaction will be negligible. Therefore, the observed decrease in absorbance at 315 nm is associated with a decrease in the dithionite concentration (Figure 2). Interestingly, the rate of the reaction does not depend on the dithionite concentration, indicating that dithionite does not participate in the rate-determining step of the catalytic process. It follows that more attention must be given to the other part of the process, viz., the reaction between $\text{Co}^{\text{I}}(\text{TSPc})^{5-}$ and nitrite, since the rate does depend on the $\text{Co}^{\text{I}}(\text{TSPc})^{5-}$ concentration as seen in Figure 2.

Reaction of $\text{Co}^{\text{I}}(\text{TSPc})^{5-}$ with Nitrite. A kinetic study was undertaken under anaerobic conditions at pH 10 and 25 °C. The ESR spectrum of the products of the reaction between $\text{Co}^{\text{I}}(\text{TSPc})^{5-}$ and an excess of NO_2^- (Figure S2, Supporting Information) is similar to that reported for $\text{Co}^{\text{II}}(\text{TSPc})^{4-}$.²² This spectrum is in agreement with that expected for a single, unpaired electron localized in the d_{z^2} orbital of a metal complex, which is essentially characteristic for low-spin octahedral $\text{Co}^{\text{II}}(\text{Pc})$ complexes.

The reaction was studied under pseudo-first-order conditions, i.e., with NaNO_2 in excess. It should be noted that an excess of NaNO_2 was maintained with respect to both $\text{Co}^{\text{I}}(\text{TSPc})^{5-}$ and dithionite, since a direct reaction between nitrite and $\text{Co}^{\text{I}}(\text{TSPc})^{5-}$ may occur when the dithionite is used up. The change in absorbance at 450 nm was used for the kinetic measurements. In this spectral region the phthalocyanine complexes of Co^{I} have a much more intensive absorption than those of Co^{II} . The shape of the absorbance/time plots at 450 nm depends on the $[\text{NaNO}_2]:[\text{Co}^{\text{I}}(\text{TSPc})^{5-}]$ ratio with nitrite in excess as shown in Figure 3.

Figure 3 demonstrates that the oxidation of $\text{Co}^{\text{I}}(\text{TSPc})^{5-}$ by nitrite exhibits an induction period, which depends on the nitrite concentration, i.e., on the rate of the redox reaction. In fact, the induction period can be related to the redox cycling of $\text{Co}^{\text{I}}(\text{TSPc})^{5-}$, during which $\text{Co}^{\text{I}}(\text{TSPc})^{5-}$ is oxidized by nitrite and the produced Co^{II} complex is reduced by the excess of dithionite present in solution. The induction period depends linearly on the selected dithionite concentration at a fixed nitrite concentration as shown in Figure 4. Once the dithionite is used up, the oxidation of $\text{Co}^{\text{I}}(\text{TSPc})^{5-}$ to $\text{Co}^{\text{II}}(\text{TSPc})^{4-}$ by nitrite can be followed as a pseudo-first-order reaction with the rate constant k_{obsd} .

The kinetics of the oxidation of $\text{Co}^{\text{I}}(\text{TSPc})^{5-}$ by nitrite depends on the selected nitrite concentration as shown in Figure 5. For nitrite concentrations up to 0.03 M, the observed rate constant first increases linearly with increasing nitrite concentration and then almost reaches a limiting value as shown by the double reciprocal plot in Figure 5a. At higher concentrations of nitrite, k_{obsd} increases further with increasing nitrite concentration as seen in Figure 5b. On the basis of these observations, it is suggested that the reaction under investigation proceeds via an inner-sphere electron-transfer reaction which involves complex formation between $\text{Co}^{\text{I}}(\text{TSPc})^{5-}$ and NO_2^- , presented in reactions 3 and 4. Although preliminary experiments showed that the band at 450 nm did not depend on the concentration of nitrite, i.e., was insensitive to the structure of the $\text{Co}^{\text{I}}(\text{TSPc})^{5-}$ complex, the changes in absorbance at 450 nm are attributed to a decrease in the concentration of the intermediate complex. The limiting rate constant reached at a nitrite concentration of approximately 0.03 M represents the electron-transfer rate constant (k_4) of the intermediate species. The increase in k_{obsd} observed at higher nitrite concentrations is ascribed to a redox path that involves a further nitrite ion as reaction partner as indicated in reactions 5 and 6.

(20) Stuzhin, P. A.; Khelevina, O. G. *Coord. Chem. Rev.* **1996**, *147*, 41.

(21) McKenna, C. E.; Gutheil, W. G.; Song, W. *Biochim. Biophys. Acta* **1991**, *1075*, 1091.

(22) (a) Rollmann L. D.; Iwamoto R. T. *J. Am. Chem. Soc.* **1968**, *90*, 1455.
(b) Rollmann L. D.; Chan S. I. *Inorg. Chem.* **1971**, *10*, 1978.

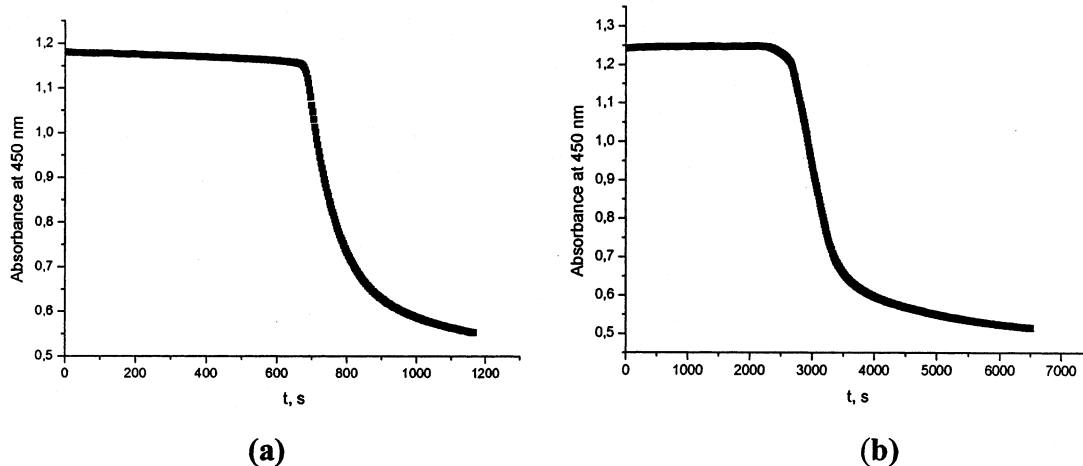


Figure 3. Time dependence of the absorbance of $\text{Co}^{\text{I}}(\text{TSPc})^{5-}$ at 450 nm during the reaction of NaNO_2 with $\text{Co}^{\text{I}}(\text{TSPc})^{5-}$, $[\text{NaNO}_2] = 8.4 \times 10^{-3}$ (a) and 3.0×10^{-2} (b) M, $[\text{Co}^{\text{I}}(\text{TSPc})^{5-}] = 7.8 \times 10^{-5}$ M, pH 10, 25 °C.

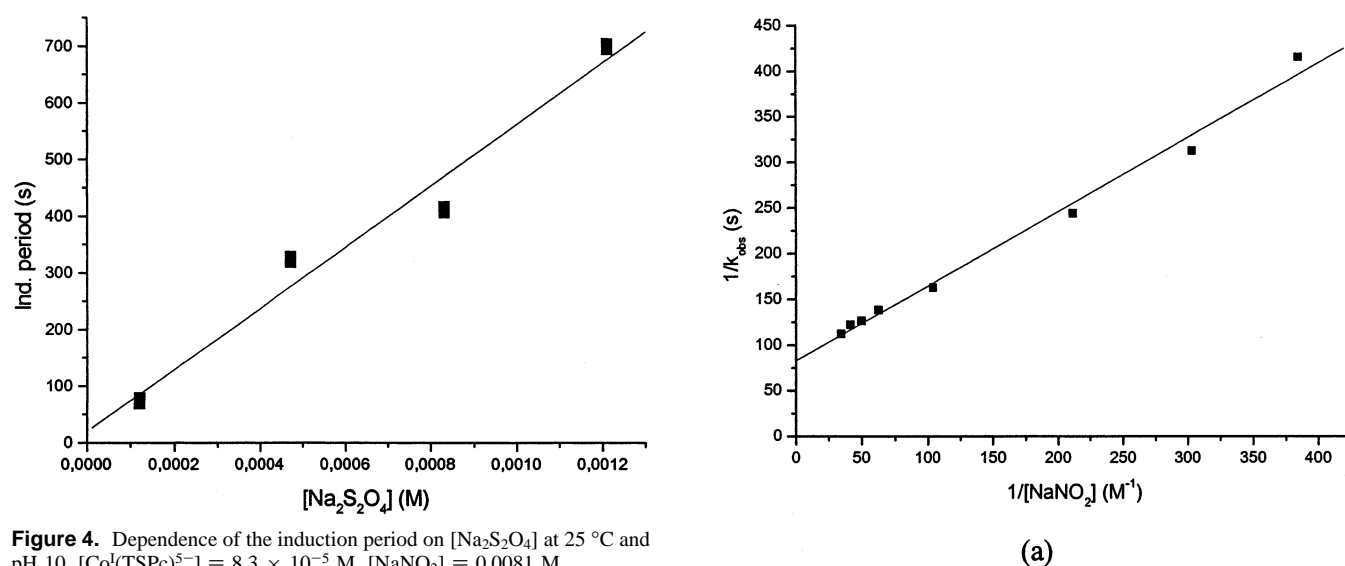
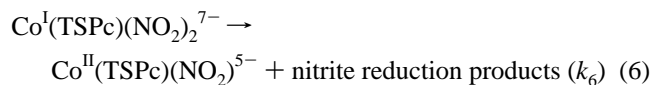
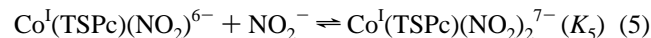
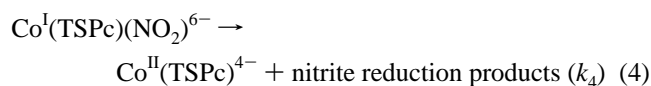


Figure 4. Dependence of the induction period on $[\text{Na}_2\text{S}_2\text{O}_4]$ at 25 °C and pH 10, $[\text{Co}^{\text{I}}(\text{TSPc})^{5-}] = 8.3 \times 10^{-5}$ M, $[\text{NaNO}_2] = 0.0081$ M.



This mechanism can qualitatively account for the complex dependence of the reaction rate on the nitrite concentration presented in Figure 5. In the low nitrite concentration range (Figure 5a), reactions 3 and 4 account for the observed kinetic behavior, and the observed first-order rate constant can be expressed as given in eq 7. The nonlinear dependence of k_{obsd} on the nitrite concentration observed in Figure 5a enables the estimation of K_3 and k_4 , which have the values $102 \pm 8 \text{ M}^{-1}$ and $0.0121 \pm 0.009 \text{ s}^{-1}$ at 25 °C and pH 10, respectively. At higher nitrite concentration, eq 7 can be reduced to $k_{\text{obsd}} = k_4$.

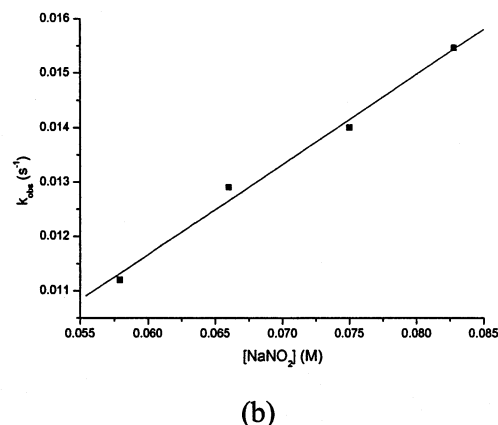


Figure 5. Dependence of the pseudo-first-order rate constant (k_{obsd} , measured following the induction period in Figure 3) on $[\text{NaNO}_2]$ at 25 °C and pH 10 for different nitrite concentration ranges: $[\text{Co}^{\text{I}}(\text{TSPc})^{5-}] = 7.8 \times 10^{-5}$ M, $[\text{Na}_2\text{S}_2\text{O}_4] = 8.1 \times 10^{-4}$ M. For the lower concentration range, the data are presented as a double reciprocal plot to demonstrate the saturation kinetics almost reached under these conditions.

$$k_{\text{obsd}} = k_4 K_3 [\text{NO}_2^-] / (1 + K_3 [\text{NO}_2^-]) \quad (7)$$

In the high nitrite concentration range (Figure 5b), reaction 4 competes with the nitrite-induced reaction path involving

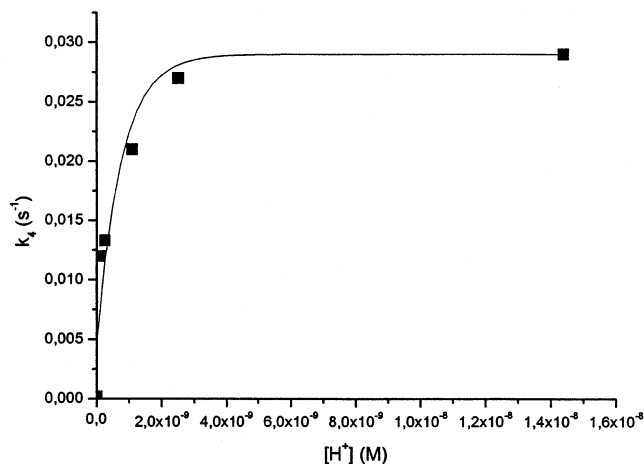


Figure 6. Dependence of k_4 on $[H^+]$ at 25 °C, $[Co^I(TSPc)^{5-}] = 7.8 \times 10^{-5}$ M, $[Na_2S_2O_4] = 6.3 \times 10^{-4}$ M.

reactions 5 and 6, for which the rate expression is given in eq 8. From the data reported in Figure 5b, a linear regression fit resulted in $k_6K_5 = 0.188 \pm 0.005$ M $^{-1}$ s $^{-1}$, which is ca. 6 times smaller than the value of k_4K_3 at pH 10.

$$k_{\text{obsd}} = k_6K_5[NO_2^-] \quad (8)$$

If k_4 is a “pure” inner-sphere electron-transfer rate constant, its value should not depend on pH. However, experiments similar to those reported in Figure 5a were performed as a function of pH and showed that k_4 (the limiting rate constant) strongly depends on pH in an alkaline medium (see Figure 6).

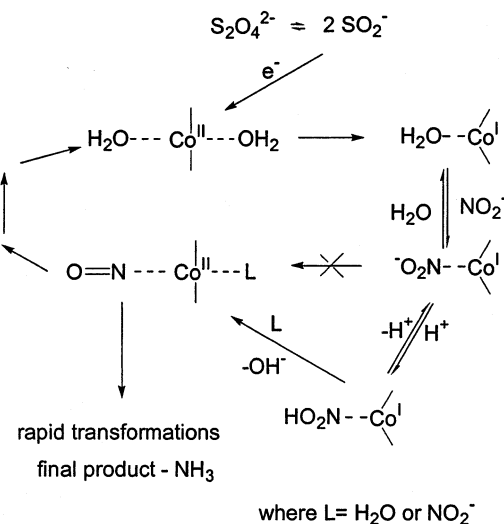
Figure 6 demonstrates that, for solutions with pH < 8.6, k_4 reaches a limiting value of 0.029 ± 0.006 s $^{-1}$. In more alkaline solutions (pH > 8.6), k_4 strongly decreases with increasing pH. This can only be due to the fact that the electron-transfer reaction is preceded by protonation of the complex such that k_4 should be expressed by eq 9, where K_a

$$k_4 = \left(\frac{K_a[H^+]}{1 + K_a[H^+]} \right) k_7 \quad (9)$$

is the protonation constant of $Co^I(TSPc)(NO_2)^{6-}$ and k_7 is the electron-transfer rate constant. At pH < 8.6, eq 9 can be simplified to $k_4 \approx k_7$ and k_7 has the value 0.029 ± 0.006 s $^{-1}$. The value of K_a was determined from the initial slope ($=K_a k_7$) of the plot in Figure 6 to be $(1.24 \pm 0.06) \times 10^8$ M $^{-1}$. This is an important result of this study, since it shows that the role of the catalyst is to shift the reaction into a more alkaline pH range, which even indicates the possibility for its realization at physiological pH. The complex in this case has the role of an electron donor to increase the electron density on the coordinated nitrite fragment. The decomposition of the protonated complex $Co^I(TSPc)(NO_2H)^{5-}$ results in the formation of $Co^{II}(TSPc)^{4-}$ and the hydronitrite radical NO_2^{\cdot} , which is known to be a product of the reduction of nitrite and rapidly decays to NO in aqueous solution.²³ We

(23) Lyman, S. V.; Schwarz, H. A.; Czapski, G. J. *J. Phys. Chem. A* **2002**, *106*, 7245.

Scheme 1. Proposed Mechanism for the Catalyzed Reduction of NO_2^- in the 0–0.03 M Concentration Range



suggest that quite a similar situation could occur in the case of natural Cu^I-containing nitrite reductases.

For more detailed mechanistic information, the thermal activation parameters were determined at pH 10 from the corresponding Eyring plots over the temperature range 15–50 °C. For reaction 4, the following parameters were found from the temperature dependence of k_4 ($=K_a k_7$) calculated from k_{obsd} at $[NaNO_2] = 0.03$ M: $\Delta H^\ddagger = 63 \pm 4$ kJ mol $^{-1}$ and $\Delta S^\ddagger = -89 \pm 11$ J K $^{-1}$ mol $^{-1}$. The complexity of the system restricts quantitative interpretation of these activation parameters. The large negative value of ΔS^\ddagger suggests a more ordered transition state as compared to the intermediate complex $Co^I(TSPc)(NO_2)^{6-}$, presumably due to electron transfer from the nonplanar Co^I complex to the planar Co^{II} complex. ¹⁵N NMR spectra showed that, in comparison to that for free ¹⁵NO₂⁻, the signal for nitrite in $Co^{II}(TSPc)(NO_2)^{5-}$ is shifted upfield by 175 ppm.

On the basis of the kinetic data, the catalytic reduction of nitrite, including formation of the Co^{II}NO complex, may be summarized as in Scheme 1.

In Scheme 1, coordination of nitrite to the Co^I complex is followed by protonation and cleavage of the N–O bond of nitrite to produce a hydroxyl group and NO bound to hexacoordinate Co^{II}. This scheme is quite similar to that mentioned above for the Cu^I-containing nitrite reductase H255N.²⁴

The composition of the reaction products at a high excess of nitrite as compared to $Co^I(TSPc)^{5-}$ ($[NaNO_2]:[Co^I(TSPc)^{5-}] = 10^4$; $[NaNO_2]:[Na_2S_2O_4] = 1:0.8$) was studied using ¹⁵N NMR and mass spectrometry. Analysis of the gas phase showed no presence of ¹⁵N-enriched products. In the ¹⁵N NMR spectra (see Figures S3 and S4 in the Supporting Information), three new signals were observed at 53, –283, and –382 ppm, respectively. The first signal corresponds to the Co^{II} complex (see above), the second to coordinated ¹⁵NH₃, and the third to free ¹⁵NH₃.²⁵ These data show that on the route from NO₂⁻ to NH₃ there is no evidence for the

(24) Boulanger, M. J.; Murphy M. E. P. *Biochemistry* **2001**, *40*, 9132.

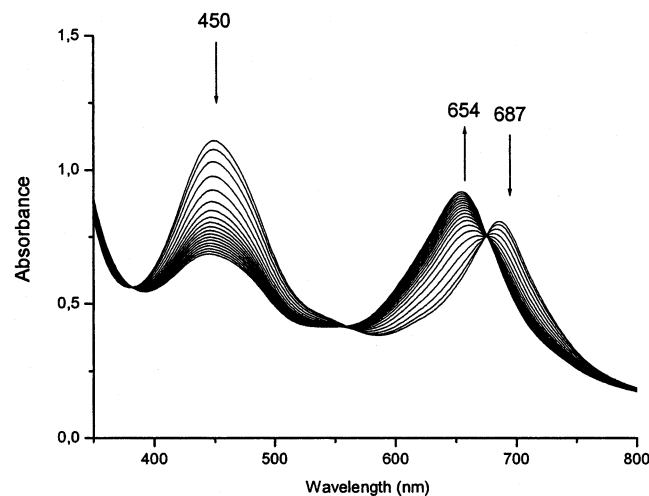


Figure 7. Spectral changes observed during the reaction of $\text{Co}^{\text{I}}(\text{TSPc})^{5-}$ with sodium nitrate, $[\text{Co}^{\text{I}}(\text{TSPc})^{5-}] = 7.8 \times 10^{-5} \text{ M}$, $[\text{NaNO}_3] = 0.32 \text{ M}$, induction period omitted for clarity, 35°C . The spectra were recorded at 120 s intervals.

formation of N_2O and N_2 under our experimental conditions. The overall reaction sequence for nitrite reduction is given by reaction 10.

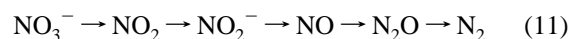


Accordingly, the second molecule of nitrite plays a catalytic role by accelerating electron transfer and breakage of the NO bond on the nitrite fragment of the intermediate complex, accompanied by formation of NO. For less excess of nitrite, the composition of the reaction products does not change, indicating no presence of N_2O and N_2 . These data show that, on variation of the excess of nitrite employed, the intermediate formation of nitric oxide can be suggested since it is reduced to ammonia, but it is not formed as a free compound since the stability constant of the $[\text{Co}^{\text{II}}(\text{TSPc}^{4-})(\text{NO})]$ complex is $1.3 \times 10^8 \text{ M}^{-1}$.²⁶

Reaction of $\text{Co}^{\text{I}}(\text{TSPc})^{5-}$ with Nitrate. The $\text{Co}^{\text{I}}(\text{TSPc})^{5-}$ complex reacts with sodium nitrate at pH 10 with formation of an EPR-active $\text{Co}^{\text{II}}(\text{TSPc})^{4-}$ species. The changes in the UV-vis spectra during the reaction are shown in Figure 7.

Similar to the reaction with nitrite, oxidation of the Co^{I} complex by nitrate is accompanied by a decrease in absorbance at 450 nm. When nitrate is used in a significant excess, the main part of the kinetic curve following the induction period, where at least 50% of the Co^{I} complex reacts, has a pseudo-zero-order character with the following activation parameters: $\Delta H^\ddagger = 128 \pm 5 \text{ kJ mol}^{-1}$ and $\Delta S^\ddagger = +77 \pm 17 \text{ J K}^{-1} \text{ mol}^{-1}$. These activation parameters cannot be interpreted in a quantitative way, although the positive value of ΔS^\ddagger may indicate that the rate-determining step involves breakage of the NO bond followed by formation of the

reaction products. It is important to note that the analysis of the products using ^{15}N NMR and mass spectrometry gave unexpected results. Contrary to those found for the reduction of nitrite, the products of the reaction between $\text{Co}^{\text{I}}(\text{TSPc})^{5-}$ and nitrate are N_2 and N_2O . Dinitrogen was detected in the gas phase and nitrous oxide in solution. The nitrogen atoms in $^{15}\text{N}_2\text{O}$ give two signals in the ^{15}N NMR spectrum (see Figure S5 in the Supporting Information) at -127.8 and -237.0 ppm (in the gas phase they have signals at -147.3 and -237.0 ppm, respectively²⁷). The observed upfield shift may be accounted for by the participation of N_2O in hydrogen bond formation. It should be noted that $^{15}\text{NH}_3$ was not observed at all. On the basis of these data, the reduction of nitrate can be represented as shown in reaction 11.



No simple kinetics was observed for this reaction (see Figures S6 and S7 in the Supporting Information). The dependence of the pseudo-zero-order rate constant (k_{obsd}) on $[\text{NaNO}_3]$ reported in Figure S7 differs significantly from that observed for nitrite in Figure 5. It may be explained in terms of different electrophilic properties of nitrite and nitrate, since the latter is a significantly more powerful electrophile with electron density being localized on the nitrogen atom. Therefore, interaction with the electron-rich Co^{I} center is more favorable in the case of nitrate, the intermediate complex $\text{Co}^{\text{I}}(\text{TSPc})(\text{NO}_3)^{6-}$ being more stable and presumably containing a $\text{Co}^{\text{I}}\text{—O}$ bond. This leads to a more pronounced catalytic effect of $\text{Co}^{\text{I}}(\text{TSPc})^{5-}$ in the reduction of nitrate since the formation of the intermediate complex proceeds more readily and does not slow the overall process. The different types of complexes formed, viz., a $\text{Co}^{\text{I}}\text{—N}$ bond for nitrite and a $\text{Co}^{\text{I}}\text{—O}$ bond for nitrate, are suggested to account for the different observed reaction products of the catalytic redox process. The hypothesis of two reaction centers in the N—O species has been confirmed recently by results from pulse radiolysis studies of nitrite.²³ It was shown that the products obtained from the reduction of nitrite ion by solvated electrons and by hydrogen atoms are not connected through a rapid protic equilibrium as previously believed. The authors assumed that the H atom quantitatively reacts by addition to the unsaturated N atom of NO_2^- , whereas the NO_2^{2-} radical is always protonated at its O atom.

Reaction of $\text{Co}^{\text{I}}(\text{TSPc})^{5-}$ with Nitrous Oxide. As reported above, N_2 and N_2O were formed during the reduction of nitrate. However, formation of N_2 is only possible if reduction of N_2O occurs under similar conditions. To investigate this further, a study was undertaken under anaerobic conditions at pH 10 and $25\text{--}50^\circ\text{C}$. N_2O -saturated buffer solutions were used in these experiments. Addition of N_2O to solutions of $\text{Co}^{\text{I}}(\text{TSPc})^{5-}$ in the presence of dithionite (reaction 12) resulted in spectral changes reported in Figure 8, which correspond to the stepwise oxidation of $\text{Co}^{\text{I}}(\text{TSPc})^{5-}$. A decrease in the peak at 450 nm and an increase in the peak at 643 nm correspond to the formation

(25) (a) Martin, G. J.; Martin, M. L.; Gouesnard, J.-P. *^{15}N NMR Spectroscopy*; Springer-Verlag: Berlin, Heidelberg, Germany, 1981; 382 pp. (b) Andersson, L.-O.; (Banus) Mason, J.; van Bronswijk, W. *J. Chem. Soc. A* **1970**, 296. (c) Chen, Y.; Lin, F.-T.; Shepherd, R. E. *Inorg. Chem.* **1999**, *38*, 973.

(26) Zilbermann, I.; Hayon, J.; Katchalski, T.; Ygdar, R.; Rishpon, J.; Shames, A. I.; Korin, E.; Bettelheim, A. *Inorg. Chim. Acta* **2000**, *305*, 53.

(27) Mastikhin, V. M.; Mudrakovsky, I. L.; Filimonova, S. V. *Chem. Phys. Lett.* **1988**, *149*, 175.

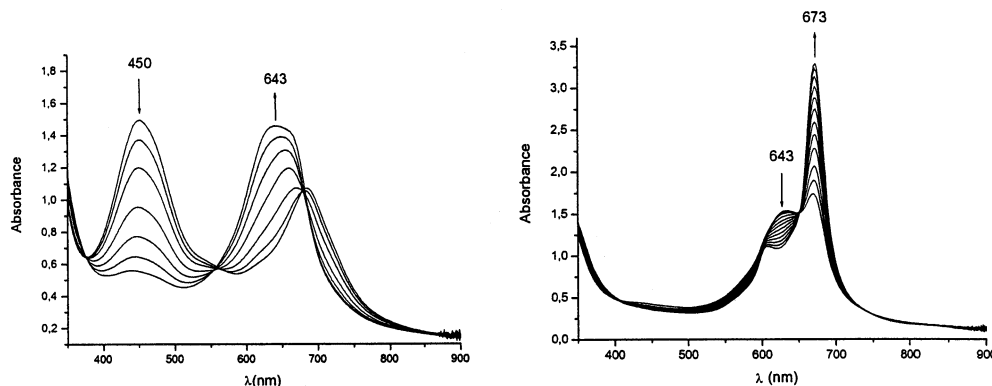
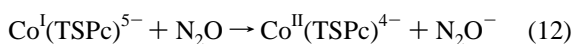
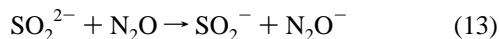


Figure 8. Spectral changes observed during the reaction of $\text{Co}^{\text{I}}(\text{TSPc})^{5-}$ with nitrous oxide, $[\text{Co}^{\text{I}}(\text{TSPc})^{5-}] = 8.3 \times 10^{-5} \text{ M}$, $[\text{N}_2\text{O}] = 1/3$ saturated, induction period omitted for clarity, 50°C . The spectra were recorded at 300 s intervals.

of the ESR-active Co^{II} complex with an ESR spectrum similar to that reported in Figure S2.



A subsequent decrease in the peak at 643 nm and an increase in the peak at 673 nm (see Figure 8) correspond to the formation of the ESR-silent Co^{III} complex. The possibility of a one-electron reduction of N_2O has been demonstrated recently by our kinetic studies on the reaction between sulfoxylate, SO_2^{2-} , and nitrous oxide in alkaline solutions²⁸ (thiourea dioxide served as the precursor of sulfoxylate). In the course of this reaction we observed the formation of dithionite, which can be explained by reaction 13 and the reverse of reaction 1.



N_2O^- is a very unstable species and decomposes immediately to OH and N_2 , which are known to be products of the reaction of N_2O and hydrated electrons.²⁹ Therefore, the observed decrease in the peak at 643 nm and an increase in the peak at 673 nm, corresponding to formation of the ESR-silent Co^{III} complex, cannot be explained by the direct interaction between $\text{Co}^{\text{II}}(\text{TSPc})^{4-}$ and N_2O^- (it should be noted that N_2O itself does not react with the Co^{II} complex). The nature of the species that oxidizes $\text{Co}^{\text{II}}(\text{TSPc})^{4-}$ is presently unknown.

Figure S8 in the Supporting Information shows that the duration of the induction period at 450 nm depends linearly on the initial concentration of dithionite. These data indicate that nitrous oxide can be reduced by dithionite in the presence of $\text{Co}^{\text{I}}(\text{TSPc})^{5-}$. Unfortunately, we could not obtain quantitative kinetic data for this reaction since the kinetic curves are extremely irreproducible (excluding induction periods) and sensitive to the initial concentrations of dithionite and N_2O (Figure S9, Supporting Information). Another complica-

tion is the fact that there are apparently no reliable methods presently available to determine N_2O in aqueous solutions.

Conclusions

Our study has clearly shown that cobalt tetrasulfophthalocyanine is an effective catalyst for the reduction of nitrite and nitrate by dithionite. The catalytic cycle includes reversible reduction of $\text{Co}^{\text{II}} \leftrightarrow \text{Co}^{\text{I}}$ and reduction of the coordinated substrate. Surprisingly, reduction of nitrite and nitrate leads to the formation of different products, although NO_2^- is an intermediate of the nitrate reduction process. This finding suggests that the structure of the complex between nitrite or nitrate and $\text{Co}^{\text{I}}(\text{TSPc})^{5-}$ determines the composition of the final reaction products. In our opinion, the most plausible structure of the intermediate complex in the case of nitrite is $\text{Co}^{\text{I}}(\text{TSPc})^{5-} \rightarrow \text{NO}_2^-$. Following protonation and inner-sphere electron transfer, the $\text{Co}^{\text{II}} \leftarrow \text{N}=\text{O}$ complex is formed, which is followed by reduction of coordinated NO and production of ammonia. Contrary to that of nitrite, ligation of nitrate presumably leads to formation of a complex with a $\text{Co}^{\text{I}}-\text{O}$ bond: $(\text{TSPc})^{5-} \text{Co}^{\text{I}} \rightarrow \text{O}=\text{NO}_2^-$. Further reduction results in the formation of the complex $(\text{TSPc})^{4-} \text{Co}^{\text{I}} \rightarrow \text{O}=\text{N}$, where NO is coordinated via oxygen. The reduction of coordinated nitric oxide gives $\text{O}=\text{N}^-$, which dimerizes and produces N_2O . Thus, N-coordination of the substrate leads to formation of ammonia, whereas O-coordination leads to the formation of nitrogen. In both processes nitric oxide is a reaction intermediate. Nitrous oxide can also be reduced under similar conditions, and this reaction may be relevant for the purification of gases containing N_2O .

Acknowledgment. We gratefully acknowledge financial support from the Deutsche Forschungsgemeinschaft (SFB 583 "Redox-Active Metal Complexes: Control of Reactivity via Molecular Architecture") and DAAD for fellowships to E.V.K. and S.V.M.

Supporting Information Available: Three ^{15}N NMR spectra and one ^1H NMR spectrum recorded during the study, one ESR spectrum, and kinetic data. This material is available free of charge via the Internet at <http://pubs.acs.org>.

IC020290F

(28) Makarov, S. V.; Kudrik, E. V.; van Eldik, R.; Naidenko, E. V. *J. Chem. Soc., Dalton Trans.* **2002**, 4074.

(29) Huie, R. E.; Clifton, C. L.; Altstein, N. *Radiat. Phys. Chem.* **1989**, *33*, 361.